change for THF photooxidation is given by[73] eq 14 where E_{ex} is

$$\Delta G = -E_{ex} + THF_{ox} - M_{red} \quad (14)$$

the energy of the longest wavelength absorption band of the metal ion-THF complex, i.e., the energy of the photon absorbed (305 nm ~ 4.1 eV), THF_{ox} is the oxidation potential of THF, and M_{red} is the reduction potential of the metal in THF. Since the "donor numbers" of THF and water are similar,[74] it is reasonable for the purpose of discussion to consider the aqueous, one-electron reduction potentials for Ag(I), Cu(I), Cu(II), and Tl(I), which are +0.80, +0.52, +0.15, and -0.34 V, respectively.[75] While the oxidation potentials of ethers are too high to allow precise measurements, a lower limit for THF_{ox} = +3.6 V can be estimated from the data available.[76] These values indicate that sufficient energy is available in the electronic excitation to render the one-electron oxidation processes highly exothermic for Ag(I) ($\Delta G \leq -1.3$ eV), Cu(I), and Cu(II) and approximately isothermic for Tl(I). The other cyclic ethers investigated all have higher ionization potentials than THF (Table II). Since the ionization and oxidation potentials of related molecules are directly correlated ($IP = aE_{D/D^+} - b$),[77] increasing ether oxidation potential renders the photooxidation process less favorable energetically.

While the mechanism of initiation of thermal polymerization of cyclic ethers by metal salts has not been investigated in detail, the absence in the present examples of metallic precipitates argues against ligand oxidation by metal ions. The possibility that trace amounts of triflic acid formed by the reaction of metal triflates with adventitious water initiate thermal polymerization can also be excluded since THF should also undergo thermal polymerization by this mechanism. The most likely mechanism for thermal polymerization is a "coordinate" mechanism in which an electron-deficient coordinated monomer is subject to nucleophillic attack by free monomer.[1,2] The metal ion thus functions as a Lewis acid polymerization initiator. Such a mechanism is known to occur in the case of catalysis of epoxide ring opening by iron, zinc, and aluminum catalysts.[2] The necessity of ether coordination for thermal polymerization is demonstrated by the inability of the Cu(I)-norbornene complex, $CuOTf \cdot C_7H_{10}$, to initiate ring opening polymerization of 1,3-dioxolane. The metal ion selectivity of thermal polymerization (Table II) may reflect the ability of Cu(I) and Cu(II) ions to form more stable etherate complexes than do Ag(I) or Tl(I) ions.

(73) Shirota, Y.; Mikawa, H. *J. Macromol. Sci., Rev. Macromol. Chem.* **1977/78**, *C16*, 129-196.
(74) Gutman, V. "The Donor-Acceptor Approach to Molecular Interactions"; Plenum Press: New York, 1978; Chapter 8.
(75) Douglas, B. E.; McDaniel, D. H. "Concepts and Models of Inorganic Chemistry"; Blaisdell: Waltham, MA, 1965; p 490.
(76) Perichon, J.; Buvet, R. *Electrochim. Acta* **1964**, *9*, 587-597.
(77) Miller, L. L.; Nordblom, G. D.; Mayers, E. A. *J. Org. Chem.* **1972**, *37*, 916-918.

Conclusions

The results of this study demonstrate that photopolymerization of THF is readily initiated by certain metal ions. Ligand-to-metal charge-transfer excitation of a metal-ether complex causes photoreduction of the metal ion and cationic polymerization of THF. When an intense broad-band source is used for irradiation, the effectiveness of the metal ion used depends solely on its oxidation state, with the 2+ ion being most effective. Following the metal ion mediated photoinitiation, polymerization proceeds through the normal cationic chain mechanism. The observed effect of anion identity on yield, the continued growth of polymer in the dark, and inhibition of polymerization by triethylamine and water are all characteristic of the thermal polymerization of THF.

Metal ion initiated photopolymerization offers several unique features not available in either thermal or organic acceptor photoinitiated systems. The THF-initiator mixture is completely stable until activated by ultraviolet light. The reacted initiator (precipitated metal) can be easily separated after polymerization by filtration. The diverse thermal and photochemical behavior observed with several different metal ions and cyclic ethers indicates that coordination may allow significant fine tuning of reactivity not achievable with thermal initiators.

Acknowledgment is made to the donors of the Petroleum Research Fund, administered by the American Chemical Society, for the generous support of this research and to PPG Industries for providing a fellowship for M.E.W. We thank the Materials Research Center of Northwestern University for access to magnetic resonance equipment supported under NSF grant DMR79-23575.

Registry No. THF, 109-99-9; $AgPF_6$, 26042-63-7; $AgBF_4$, 14104-20-2; $AgSbF_6$, 26042-64-8; AgOTf, 2923-28-6; $Cu(OTf)_2$, 34946-82-2; TlOTf, 73491-36-8; CuOTf, 42152-44-3; cyclohexene oxide, 286-20-4; oxetane, 503-30-0; 1,3-dioxolane, 646-06-0; 1,3,5-trioxane, 110-88-3.

Orientation and Linear Dichroism of Symmetrical Aromatic Molecules Imbedded in Stretched Polyethylene

Erik W. Thulstrup*[1] and Josef Michl*

Contribution from the Department of Chemistry, University of Utah, Salt Lake City, Utah 84112. *Received January 18, 1982*

Abstract: A general procedure for the analysis of linear dichroism of solutes partially aligned in a stretched polymer is described. Results for UV-visible dichroism of over a hundred symmetrical aromatic molecules in polyethylene are presented. Their orientation factors are dominated primarily by molecular shape, making the experimentally very simple stretched-sheet method suitable for the determination of absolute polarization directions in aromatics.

The determination of polarization directions of electronic transitions in molecules has been acquiring increasing importance,[2,3] particularly in biochemical applications. Because of its experimental simplicity, the stretched-sheet method of UV-visible[2-4] and IR[5] polarization measurement is gaining in popularity. In the method, the solute of interest is imbedded in a stretched polymer sheet, which orients it partially, and its linear dichroism is then measured and evaluated. Qualitative observations of this phenomenon were reported a hundred years ago,[6] and the several

(1) Permanent address: Department of Chemistry, Royal Danish School of Educational Studies, Copenhagen, Denmark.
(2) Nordén, B. *Appl. Spectrosc. Rev.* **1978**, *14*, 157.
(3) For additional references, see: Thulstrup, E. W. "Aspects of the LD and MCD of Planar Organic Molecules"; Springer-Verlag: Heidelberg; 1980.
(4) Thulstrup, E. W.; Michl, J. *J. Phys. Chem.* **1980**, *84*, 82.
(5) Radziszewski, J. G.; Michl, J. *J. Phys. Chem.* **1981**, *85*, 2934.
(6) Ambronn, H. *Ber. Dtsch. Bot. Ges.* **1888**, *6*, 85, 226; *Ann. Phys. (Leipzig)* **1888**, *34*, 340.

0002-7863/82/1504-5594$01.25/0

quantitative evaluation procedures currently in use have recently been critically compared.[4]

The purpose of the present paper is twofold. First, we provide a full account of a generalized version of the linear dichroism evaluation procedure for partially aligned symmetrical molecules in uniaxial samples proposed in 1965–1970 by Eggers et al.[7-9] (the TEM model); for a recent extension of the treatment to processes involving two photons, such as polarized fluorescence and Raman spectroscopy of partially oriented uniaxial samples, see ref 10. Second, we present experimental results for the orientation of about a hundred symmetrical aromatic molecules, demonstrating a close relation between molecular shape and orientation factors. In this context a "symmetrical molecule" is one in which no two of the symmetry-adapted molecular axes x, y, and z transform according to the same one-dimensional irreducible representation. The experimental results for the orientation factors of symmetrical molecules can be used to estimate the orientation factors for other aromatic molecules, including those of lower symmetry such as C_{2h} or C_s. Their knowledge is a prerequisite for the determination of the polarization directions for such molecules by measurement of linear dichroism. The collection of data also provides a background for attempts to unravel the presently poorly understood mechanism of solute orientation in polymers.

Experimental Section

The compounds used in the measurements were commercial or obtained as gifts from various sources. They were purified by gradient sublimation as required. The measurement procedures were described in ref 8. Solutions in spectral grade chloroform were used to swell the polyethylene sheets, which had been stretched to about 600%. Over the years, linear low-density polyethylene sheets from several commercial sources were used, with relatively little effect on the molecular orientation. The effects were somewhat larger when noncommercial sheets made according to ref 5 were used. The spectra were recorded on a Cary 17 instrument for two mutually perpendicular positions of a Glan polarizer located at 45° from the vertical, one with the electric vector of the light parallel and one perpendicular to the stretching direction of the sheet. A second polarizer was placed in the reference compartment. The spectra were digitized and base lines obtained from undoped polyethylene sheets were subtracted by computer.

Results and Discussion

In the following, we first provide a full general description of the TEM procedure for the evaluation of dichroic spectra (section 1). Then, we provide a visual representation of the orientation factors and discuss their relation to molecular shape (section 2).

(1) The TEM Model. (1.1) Assumptions. This model for evaluation of linear dichroism of partially oriented molecular assemblies is based on three assumptions. First, the orienting medium is assumed to be uniaxial, i.e., it has a unique axis Z and all directions perpendicular to Z are equivalent among themselves. There is reasonable evidence that this assumption is fulfilled in media such as stretched polyethylene[9] and nematic liquid crystals.[11]

Second, the anisotropy of solvent effects is assumed to be negligible. The transition energies and transition moments relative to the molecular framework are taken to be independent of the molecular orientation, and the effect of the solvent on local electric fields produced by incident electromagnetic radiation is taken to be isotropic. Although this assumptions is certainly not fulfilled exactly, there is little doubt that it is acceptable for strong transitions in weakly birefringent materials within the presently required accuracy.[12] For work in strongly birefringent solvents such as certain liquid crystals, this assumption may no longer be acceptable, and the measured polarized spectra will then have to be multiplied by suitable correction factors.[13]

Third, it is assumed that recognizable, intrinsically purely polarized spectral features (peaks, shoulders) can be found somewhere in the accessible region of the absorption spectrum. These features may mutually overlap in an incoherent fashion. If nonoverlapping purely polarized transitions can be found, the evaluation is particularly easy. Even if all such features do overlap others of different polarization, the evaluation is feasible as long as they do not have nearly identical spectral shapes and locations. In this instance, the stepwise reduction method[4,8] is used as described below. In principle, one can justify the assumption of purely polarized spectral features rigorously only if independent information is available from other measurements (e.g., single crystal data or fluorescence polarization). However, it appears quite reasonable to assume that peaks in vibrational spectra and the zero–zero peaks of relatively intense bands in UV–visible spectra of rigid molecules of high symmetry (D_{2h}, C_{2v}) are purely polarized along one of the symmetry axes. This must be true unless the symmetry-lowering effects of solute–solvent interactions are strong (unlikely for intense transitions, particularly for solutes in the nonpolar polyethylene), unless vibronic intensity borrowing by extremely low frequency vibrations intervenes in electronic transitions (uncommon in rigid molecules), or unless the excitation energies of two independent transitions of different polarizations happen to coincide exactly. In the case of pyrene, this assumption was recently checked by a comparison of linear dichroism in the UV and IR regions.[5] It should be noted that the assumption that at least one observable spectral feature is intrinsically purely polarized is common to all methods for analyzing the linear dichroism of partially aligned samples unless the second moments of the orientation distribution function are known in advance.

(1.2) Measurements. Let us associate the uniaxial anisotropic sample with a system of axes X, Y, and Z such that Z coincides with the unique axis (polymer stretching direction). Optical density measured as a function of wavelength λ with the electric vector of the light oriented parallel to Z, $E_Z'(\lambda)$, and that measured with the electric vector oriented perpendicular to Z, $E_X'(\lambda) = E_Y'(\lambda)$, are determined and corrected for the base lines due to polymer absorption and scattering, $E_Z^0(\lambda)$ and $E_X^0(\lambda) = E_Y^0(\lambda)$, respectively. Traditionally, the orientation of the light beam is perpendicular to Z, and the corrected curves $E_Z(\lambda) = E_Z'(\lambda) - E_Z^0(\lambda)$ and $E_Y(\lambda) = E_Y'(\lambda) - E_Y^0(\lambda)$ are obtained with two perpendicular orientations of a polarizer, but other arrangements are possible. For instance, since the sample is uniaxial, the $E_Y(\lambda)$ curve can be equally well obtained without a polarizer, with the light beam parallel to Z. Measurements with the beam parallel to Z would be difficult on a stretched polymer sheet of the usual thickness. We have performed them on thin disks cut from a stretched polymer rod; they are commonly performed on liquid crystals.[14]

Any two independent linear combinations of $E_Z(\lambda)$ and $E_Y(\lambda)$ can be determined instead, for instance, their sum and difference. Often, the notations $E_\parallel(\lambda)$ and $E_\perp(\lambda)$ are used for the presently

(7) Thulstrup, E. W.; Eggers, J. H. Lectures at the 8th European Congress on Molecular Spectroscopy, Copenhagen, 1965; *Chem. Phys. Lett.* **1968**, *1*, 690.

(8) Thulstrup, E. W.; Michl, J.; Eggers, J. H. *J. Phys. Chem.* **1970**, *74*, 3868.

(9) Michl, J.; Thulstrup, E. W.; Eggers, J. H. *J. Phys. Chem.* **1970**, *74*, 3878.

(10) Michl, J.; Thulstrup, E. W. *J. Chem. Phys.* **1980**, *72*, 3999. See also: Thulstrup, E. W.; Michl, J. *J. Mol. Struct.* **1980**, *61*, 175.

(11) Meier, G.; Sackmann, E.; Grabmaier, J. G. "Applications of Liquid Crystals"; Springer-Verlag: Heidelberg, 1975.

(12) Even in a single crystal of polyethylene, the birefringence is only a few percent in the visible range: Bunn, C. W.; deDaubery, R. *Trans. Faraday Soc.* **1954**, *50*, 1173. The anisotropic local-field effects have been investigated by measuring the induced circular dichroism of cubic molecules in cholesteric media and have been found to be extremely weak. For leading references, see: Samori, B. *J. Phys. Chem.* **1979**, *83*, 375. Dudley, R. J.; Mason, S. F.; Peacock, R. D. *J. Chem. Soc., Faraday Trans. 2* **1975**, 997. Evidence for a detectable distortion of the polarization of the very weak origin of the L_b transition of pyrene away from the symmetry axis by the anisotropic interaction with the surrounding molecules of a nonpolar solvent (stretched polyethylene or solid 3-methylpentane) has now been obtained (Langkilde, F. W.; Gisin, M.; Thulstrup, E. W.; Michl, J., unpublished results). All detectable effects disappear when the intrinsic intensity of the L_b origin is increased by symmetric substitution. Thus, all the evidence available at present suggests that the neglect of the anisotropy of solvent effects is justified for strong transitions in reasonably well oriented samples.

(13) For a discussion of solvent effects on solute transition probabilities, see: Myers, A. B.; Birge, R. R. *J. Chem. Phys.* **1980**, *73*, 5314.

(14) Kelker, H.; Hatz, R.; Wirzing, G. *Fresenius Z. Anal. Chem.* **1973**, *267*, 161. Fernandes, J. R.; Venugopalan, S. *Chem. Phys. Lett.* **1978**, *53*, 407.

defined $E_Z(\lambda)$ and $E_Y(\lambda)$, respectively. The measurement of $E_Z(\lambda)$ and $E_Y(\lambda)$, and, particularly, the direct measurement of their difference,[2] can be performed quite accurately. We believe that the main source of remaining experimental uncertainty is the subtraction of the base line, particularly at short wavelengths.

(1.3) Basic Theory. In the following, lower-case letters are used for molecule-fixed coordinate axes x, y, and z. Unit vectors along directions U and u are denoted **U** and **u**, respectively. The coordinates of a general vector **R** in the sample-fixed system are R_X, R_Y, R_Z, while in the molecule-fixed system they are R_x, R_y, and R_z. The angles between R and the sample-fixed axes are R^X, R^Y, R^Z and those between R and the molecular axes are R^x, R^y, and R^z.

Let the absorption of interest be due to molecules of arbitrary symmetry imbedded in the uniaxial medium. Let $\mathbf{M}(i)$ be the electric dipole transition moment of the ith molecular transition, $g_i(\lambda)$ its line-shape function, and ϵ the direction of the electric field of the incident linearly polarized light. If the effects of the birefringence of the samples are negligible and, particularly, if ϵ coincides with Z or is perpendicular to it, the transmittance $T_\epsilon'(\lambda)$, uncorrected for base line, is given by

$$T_\epsilon'(\lambda) = \sum_{U=X,Y,Z} (\cos^2 \epsilon^U) \times 10^{|-\kappa(\lambda)f(\lambda)cl\sum_i g_i(\lambda)\langle[\mathbf{U}\cdot\mathbf{M}(i)]^2\rangle - E_U^0(\lambda)|} \quad (1)$$

where the summation over i runs over all transitions, the pointed brackets indicate averaging over all molecules in the lightpath of length l (cm), the molar solute concentration is c, $\kappa(\lambda) = 3.27 \times 10^{11}/\lambda$ (λ in nm), and the function $f(\lambda)$ represents the modification of the absorption probability by the presence of solvent molecules. It depends on factors such as the refractive index of the solvent[13] and, strictly speaking, also on U, but as noted above, the anisotropy in solvent effects will be assumed to be negligible in the present treatment. A generalization to the case in which $f_U(\lambda)$ depends significantly on U is straightforward and particularly simple in the case of samples of low optical density as long as a suitable approximation for $f_U(\lambda)$ is available (cf. ref 13).

We use

$$\langle[\mathbf{U}\cdot\mathbf{M}(i)]^2\rangle = |\mathbf{M}(i)|^2\langle\cos^2 M^U(i)\rangle \quad (2)$$

and introduce the definition

$$K_i = \langle\cos^2 M^Z(i)\rangle \quad (3)$$

Using the facts that the squares of the direction cosines of a vector add up to 1 and that $\langle\cos^2 M^X(i)\rangle = \langle\cos^2 M^Y(i)\rangle$ since the sample is uniaxial, we obtain

$$T_\epsilon'(\lambda) = (\cos^2 \epsilon^Z) \times 10^{-|\kappa(\lambda)f(\lambda)cl\sum_i g_i(\lambda)|\mathbf{M}(i)|^2K_i + E_Z^0(\lambda)|} + (\cos^2 \epsilon^Y + \cos^2 \epsilon^X) \times 10^{-|\kappa(\lambda)f(\lambda)cl\sum_i g_i(\lambda)|\mathbf{M}(i)|^2(1-K_i)/2 + E_Y^0(\lambda)|} \quad (4)$$

Let us define $A(i,\lambda)$ as three times the contribution of the ith transition to the absorbance measured on an isotropic sample, for which $K_i = {}^1/_3$ for any i:

$$A(i,\lambda) = \kappa(\lambda)f(\lambda)cl g_i(\lambda)|\mathbf{M}(i)|^2 \quad (5)$$

Then, the result for polarized transmittance measured with the polarizer in an arbitrary orientation ϵ is

$$T_\epsilon'(\lambda) = (\cos^2 \epsilon^Z) \times 10^{-|\sum_i A(i,\lambda)K_i + E_Z^0(\lambda)|} + (\sin^2 \epsilon^Z) \times 10^{-|\sum_i A(i,\lambda)(1-K_i)/2 + E_Y^0(\lambda)|} \quad (6)$$

The measurement of the base line yields

$$T_\epsilon^0(\lambda) = (\cos^2 \epsilon^Z) \times 10^{-E_Z^0(\lambda)} + (\sin^2 \epsilon^Z) \times 10^{-E_Y^0(\lambda)} \quad (7)$$

In an isotropic solution, $K_i = {}^1/_3$ and $E_Z^0(\lambda) = E_Y^0(\lambda)$. The expected result is then obtained for the base-line corrected absorbance $E_\epsilon^{iso}(\lambda)$:

$$E_\epsilon^{iso}(\lambda) = -\log [T_\epsilon'(\lambda)/T_\epsilon^0(\lambda)] = E^{iso}(\lambda) = ({}^1/_3)\sum_i A(i,\lambda) \quad (8)$$

A similar result is obtained for an oriented sample if the polarization direction ϵ forms the "magic angle" (54.7°) with the unique axis Z. This can be accomplished by using a beam propagating in a direction perpendicular to Z as long as birefringence is negligible and the sample is optically thin so that the induced ellipticity and the rotation of ϵ by the dichroic absorption can be neglected. It can be more realistically accomplished by propagating the light beam through an optically thin sample at the magic angle to the Z axis, with its polarization direction contained in the plane formed by the Z axis and the light propagation direction. In such cases, $\cos^2 \epsilon^Z = {}^1/_3$ and $\sin^2 \epsilon^Z = {}^2/_3$, and expansion of the exponentials in (6) yields an expression first order in $A(i,\lambda)$ and in the $E_U^0(\lambda)$'s

$$E_{magic}(\lambda) = -\log [T_{magic}'(\lambda)/T_{magic}^0(\lambda)] = E^{iso}(\lambda) \quad (9)$$

For the particular polarizer alignments of interest here, parallel or perpendicular to Z, the general expression (6) simplifies to

$$\begin{pmatrix} E_X(\lambda) \\ E_Y(\lambda) \\ E_Z(\lambda) \end{pmatrix} = \sum_i A(i,\lambda) \begin{pmatrix} (1-K_i)/2 \\ (1-K_i)/2 \\ K_i \end{pmatrix} \quad (10)$$

which displays the expected uniaxial symmetry, $E_X(\lambda) = E_Y(\lambda)$.

Equation 10 is the basis of the TEM model. The general strategy now is to obtain the orientation factors K_i for the individual transition moments $\mathbf{M}(i)$ from the experimental curves $E_Y(\lambda)$ and $E_Z(\lambda)$, and this will be discussed in section 1.4. Then, the two fundamental problems can be addressed: (a) the orientation of $\mathbf{M}(i)$ within the molecular framework and (b) the average alignment of the molecular framework with respect to the sample axis Z. In molecules of sufficient symmetry, the solution of the problems is easy, and we shall deal with this class of solutes in section 1.5. The situation is more complex for low-symmetry molecules, as discussed in section 1.6.

(1.4) Evaluation of the Orientation Factors. Equation 10 shows that spectral features polarized along the direction of $\mathbf{M}(i)$ will be eliminated in the following linear combination of $E_Z(\lambda)$ and $E_Y(\lambda)$:

$$E_Z(\lambda) - \frac{2K_i}{1-K_i} E_Y(\lambda) \quad (11)$$

The experiments that determine some linear combinations of $E_Z(\lambda)$ and $E_Y(\lambda)$ can be evaluated similarly. Measurements in which the polarization of light propagating along X is modulated between the Y and Z directions[2] produce an ac signal that yields, after subtraction of the base line, directly the linear dichroism

$$LD(\lambda) = E_Z(\lambda) - E_Y(\lambda) \quad (12)$$

This can be combined with $E_{Y,Z}(\lambda)$, defined as

$$E_{Y,Z}(\lambda) = [E_Z(\lambda) + E_Y(\lambda)]/2 \quad (13)$$

which can be obtained from the dc signal generated in the same modulated measurement, again corrected for the base line. Alternatively, $E_{Y,Z}(\lambda)$ can be obtained from a base-line corrected measurement of the optical density of the oriented sample $D(\lambda)$ with a beam of unpolarized light propagating along X, by using

$$E_{Y,Z}(\lambda) = D(\lambda) + \log \frac{10^{[LD(\lambda)+\Delta(\lambda)]/2} + 10^{-[LD(\lambda)+\Delta(\lambda)]/2}}{10^{\Delta(\lambda)/2} + 10^{-\Delta(\lambda)/2}} \quad (14)$$

where the correction curve $\Delta(\lambda)$ is given by

$$\Delta(\lambda) = E_Z^0(\lambda) - E_Y^0(\lambda) \quad (15)$$

When $\Delta(\lambda)$ is neglected and the relation $E^{iso}(\lambda) = E_{Y,Z}(\lambda) - LD(\lambda)/6$ is used, (14) simplifies to the form given in ref 2.

In order for the reduction to be performed on the curves $LD(\lambda)$ and $E_{Y,Z}(\lambda)$, the appropriate linear combination to seek is

$$LD(\lambda) - 2\frac{3K_i - 1}{K_i + 1} E_{Y,Z}(\lambda) \quad (16)$$

Linear dichroism can also be measured by using only unpolarized light, for instance, recording $E_Y(\lambda)$ with a beam propagating along the Z axis of the oriented sample and $E^{iso}(\lambda)$ with a beam passing through an unoriented sample with the same number of molecules in the light beam. Such measurements have been performed by using a nematic liquid crystal as the orienting

medium and then repeating the measurement above the isotropic melting point.[14] The appropriate linear combinations for the determination of K_i are again derived easily.

The determination of the orientation factors K_i according to (11) is very simple when purely polarized spectral regions can be found. With a purely polarized transition i located at λ_i, the sum in (10) is reduced to a single term at λ_i and we obtain

$$\frac{E_Z(\lambda_i)}{E_Y(\lambda_i)} = \frac{2K_i}{1-K_i} \tag{17}$$

so that

$$K_i = \frac{E_Z(\lambda_i)}{E_Z(\lambda_i) + 2E_Y(\lambda_i)} = \frac{E_Z(\lambda_i)}{3E^{iso}(\lambda_i)} = \frac{3E^{iso}(\lambda_i) - 2E_Y(\lambda_i)}{3E^{iso}(\lambda_i)} \tag{18}$$

In most molecules this fortunate situation occurs only for a few UV–visible transitions, and in many molecules for none. However, this does not prevent an accurate determination of the orientation factors as long as mutually overlapping but intrinsically purely polarized spectral features can be recognized. The method used in such cases is the stepwise reduction procedure.[8] This method is somewhat similar to the determination of the composition of a mixture from its absorption spectrum and those of its components. Linear combinations of $E_Z(\lambda)$ and $E_Y(\lambda)$ are constructed for a series of values of d, $E_Z(\lambda) - dE_Y(\lambda)$. According to (10), these curves are given by

$$E_Z(\lambda) - dE_Y(\lambda) = \sum_i [K_i - d(1 - K_i)/2]A(i,\lambda) \tag{19}$$

and consist of a sum of terms corresponding to the individual transitions i, whose relative weight can be varied arbitrarily by the choice of d. Now, d is determined so that all spectral features associated with transition i just disappear from the combination. This happens when the coefficient of $A(i,\lambda)$ in (14) vanishes, say, for $d = d_i$. Then,

$$K_i = d_i/(2 + d_i) \tag{20}$$

Figure 1 shows an example of stepwise reduction. The UV–visible absorption spectrum of benzo[*rst*]pentaphene[15] (**9**) contains a large number of electronic transitions. We note that the peaks near 30 000, 37 000, and 45 000 cm^{-1} all disappear from the linear combination $E_Z(\lambda) - d_1E_Y(\lambda)$ when d_1 approaches the value 0.4. Similarly, the 0–0 vibronic peak of the first transition at 25 000 cm^{-1} and the peaks at 34 000 and 41 000 cm^{-1} all disappear from the curve $E_Y(\lambda) - (1/d_2)E_Z(\lambda)$ when $(1/d_2)$ approaches the value 0.2. Clearly, the transitions in each group share a common value of K_i. As will be discussed in more detail in the following section, this is a reflection of molecular symmetry that only permits π,π^* transition moments along the short and the long in-plane symmetry axes of the molecule. The optimum values of d_1 and d_2 yield the K_i values of 0.19 and 0.75 for the first and the second group of transitions, respectively.

(1.5) High-Symmetry Molecules. In this section we shall specialize the treatment for molecules of point group symmetry such that the molecular axes x, y, and z belong to different irreducible representations (two of them may belong to the same degenerate representation), e.g., C_{2v} or D_{2h}. This has two simplifying effects. First, if the assumptions listed in section 1 hold, transition moments $M(i)$ can only lie in the molecular axes determined by symmetry, x, y, and z (the components of a degenerate state i can be chosen so that this is true). Second, the orientation distribution is symmetrical, and the axes x, y, and z are the principal axes of the orientation tensor[4] with elements

$$K_{uv} = \langle \cos u^Z \cos v^Z \rangle \tag{21}$$

so that in this case

$$K_{uv} = \delta_{uv}K_{uu}, \qquad u = x, y, z \tag{22}$$

where $K_{uu} = K_u$ is identical with the K_i defined in (3) if $\mathbf{M}(i)$ is directed along the axis u.

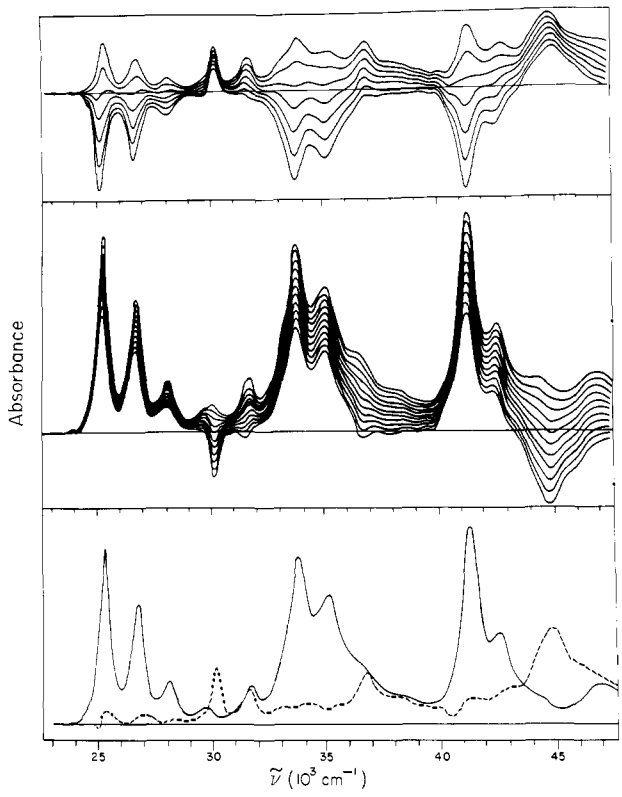

Figure 1. Stepwise reduction of the UV linear dichroic spectra of benzo[*rst*]pentaphene (**9**) in stretched polyethylene. Absorbance is plotted vertically. (Bottom) Reduced spectra: $E_Z(\lambda) - 0.47E_Y(\lambda)$ (full line) and $E_Y(\lambda) - 0.17E_Z(\lambda)$ (dashed line). (Center) Family of curves $E_Z(\lambda) - d_1E_Y(\lambda)$ with d_1 increasing from 0.0 (top) to 2.0 (bottom) in steps of 0.2. (Top) Family of curves $E_Y(\lambda) - (1/d_2)E_Z(\lambda)$ with $1/d_2$ increasing from 0.0 (top) to 0.6 (bottom) in steps of 0.1.

The procedure for deriving the three K_u's has been checked on molecules with three transitions whose moment directions did not lie in the same plane.[5,16,17] If molecular symmetry dictates an additional relation between the K_u's, only one linear combination needs to be found.

The use of the K_u's for the description of the orientation distribution offers the advantage of simple physical interpretation and of simple formulas. Other equivalent descriptions are in use and are discussed in ref 4.

Having shown how the orientation factors K_u can be determined, we next address the problem of finding the reduced spectra $A_u(\lambda)$, $u = x, y, z$. This is essential for the analysis of the spectrum in terms of the location and number of independent transitions, their polarizations, and fine structure.

For symmetrical molecules we define the reduced spectrum $A_u(\lambda)$ for the direction u as the sum of the contributions $A(i,\lambda)$ from all transitions i polarized along u:

$$A_u(\lambda) = \sum_{i:u} A(i,\lambda) \tag{23}$$

The general expression 10 for polarized absorbance now becomes

$$\begin{pmatrix} E_Y(\lambda) \\ E_Z(\lambda) \end{pmatrix} = \begin{pmatrix} {}^1/_2(1-K_z) & {}^1/_2(1-K_y) & {}^1/_2(1-K_x) \\ K_z & K_y & K_x \end{pmatrix} \begin{pmatrix} A_z(\lambda) \\ A_y(\lambda) \\ A_x(\lambda) \end{pmatrix} \tag{24}$$

As illustrated by Figure 1, in symmetrical molecules the K_i values obtained simply from dichroic ratios or less simply by the stepwise reduction procedure can only be identical with one of the three orientation factors of the molecular axes K_x, K_y or K_z.

(15) Pedersen, P. B.; Thulstrup, E. W.; Michl, J. *Chem. Phys.* **1981**, *60*, 187.

(16) Michl, J.; Thulstrup, E. W. *Spectrosc. Lett.* **1977**, *10*, 401.

(17) Thulstrup, E. W.; Spanget-Larsen, J.; Gleiter, R. *Mol. Phys.* **1979**, *37*, 1381.

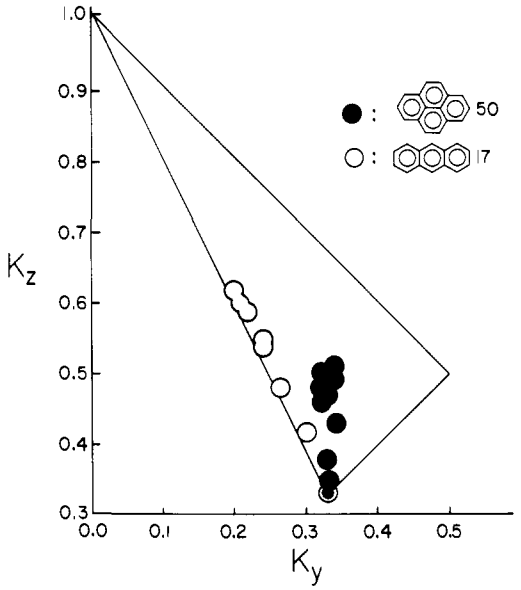

Figure 2. Reduction factors for pyrene (**50**) and anthracene (**17**) in stretched polyethylene for various degrees of stretching.

It is clear that it is impossible to determine three linearly independent curves, $A_x(\lambda)$, $A_y(\lambda)$, and $A_z(\lambda)$, from the two independent experimental curves $E_Z(\lambda)$ and $E_Y(\lambda)$ in the absence of additional information. The most obvious remedy is to find a third spectrum, linearly independent of $E_Z(\lambda)$ and $E_Y(\lambda)$. Then, a generalization of (24) with a 3 × 3 matrix of orientation factors will provide the three sought spectra $A_u(\lambda)$ once the matrix is inverted. A linearly independent third curve cannot be any other absorption spectrum measured on the same uniaxial sample nor the isotropic solution absorption spectrum [cf. (8)]. In principle, it might be possible to use a solution in the same polymer uniaxially stretched to a different degree, or, if solvent effects are negligible, a solution in a different uniaxial anisotropic medium. If the orientation factors in the new oriented sample are K_u^*, the new spectra $E_Z^*(\lambda)$ and $E_Y^*(\lambda)$ will be linearly independent of $E_Z(\lambda)$ and $E_Y(\lambda)$, and therefore useful only if

$$(K_z^* - \tfrac{1}{3})/(K_y^* - \tfrac{1}{3}) \neq (K_z - \tfrac{1}{3})/(K_y - \tfrac{1}{3}) \quad (25)$$

A geometrical representation of this result can be provided: the straight line going through points (K_z, K_y) and (K_z^*, K_y^*) must not pass through the point $(\tfrac{1}{3}, \tfrac{1}{3})$. We shall return to a geometrical representation of the K's below.

The possibility that several different degrees of stretching of the same polymer could be used does not look very promising. Some results for polyethylene are shown in Figure 2, and it is clear that all points (K_z, K_y) lie near a line passing through the isotropic point, so that the two sides of inequality 25 are almost equal. Similar results have been obtained in poly(vinyl alcohol).[18] If other molecules behave similarly as those investigated so far, the determination of three independent $A(\lambda)$'s by this approach will generally be impossible or at least very inaccurate. The use of two different polymers is more promising.

There are three special cases in which reduced spectra can be obtained from only two measured curves $E_Z(\lambda)$ and $E_Y(\lambda)$. Fortunately, these occur very commonly in practice, thereby making the method widely applicable.

(i) If the orienting properties of the z and y axes are equal (e.g., disk-shaped molecules), $K_z = K_y = (1 - K_x)/2$, and $[A_z(\lambda) + A_y(\lambda)]$ and $A_x(\lambda)$ can be obtained separately:

$$[A_z(\lambda) + A_y(\lambda)]/2 = [K_zE_Z(\lambda) - (1 - 2K_z)E_Y(\lambda)]/(3K_z - 1)$$
$$= [(1 - K_x)E_Z(\lambda) - 2K_xE_Y(\lambda)]/(1 - 3K_x) \quad (26)$$

$$A_x(\lambda) = [2K_zE_Y(\lambda) - (1 - K_z)E_Z(\lambda)]/(3K_z - 1)$$
$$= [2(1 - K_x)E_Y(\lambda) - (1 + K_x)E_Z(\lambda)]/(1 - 3K_x) \quad (27)$$

(ii) If the orienting properties of the y and x axes are equal (e.g., rod-shaped molecules), $K_z = (1 - K_y)/2$, $K_y = K_x$, and $A_z(\lambda)$ and $[A_y(\lambda) + A_x(\lambda)]$ can be obtained separately:

$$A_z(\lambda) = [(1 + K_z)E_Z(\lambda) - 2(1 - K_z)E_Y(\lambda)]/(3K_z - 1)$$
$$= [(3 - K_y)E_Z(\lambda) - 2(1 + K_y)E_Y(\lambda)]/(1 - 3K_y) \quad (28)$$

$$[A_y(\lambda) + A_x(\lambda)]/2 = [2K_zE_Y(\lambda) - (1 - K_z)E_Z(\lambda)]/(3K_z - 1)$$
$$= [2(1 - K_y)E_Y(\lambda) - (1 + K_y)E_Z(\lambda)]/(1 - 3K_y) \quad (29)$$

If the orienting properties of all three axes are equal ($K_z = K_y = K_x = \tfrac{1}{3}$), no useful orientation results, and the reduction cannot be performed.

(iii) If a spectral region can be found in which one of the three components $A_z(\lambda)$, $A_y(\lambda)$, or $A_x(\lambda)$ is negligibly small, the other two components can be determined in this region. For instance, in many aromatic molecules, out-of-plane polarized intensity is negligible in the visible and near-UV regions; i.e., $A_x(\lambda) = 0$. Then,

$$A_z(\lambda) = [(1 - K_y)E_Z(\lambda) - 2K_yE_Y(\lambda)]/(K_z - K_y) \quad (30)$$

$$A_y(\lambda) = [2K_zE_Y(\lambda) - (1 - K_z)E_Z(\lambda)]/(K_z - K_y) \quad (31)$$

It is seen that the purely polarized spectra $A_z(\lambda)$ and $A_y(\lambda)$ are proportional to the curves given by (11), using K_z and K_y, respectively, for K_i. These curves are shown in the bottom part of Figure 1 and are the "correctly reduced" linear combinations of $E_Z(\lambda)$ and $E_Y(\lambda)$ from which the values of the K_u's were obtained. Note that the proportionality constants are not the same for $A_z(\lambda)$ and $A_y(\lambda)$.

(1.6) Low-Symmetry Molecules. We shall now return to the general case of low-symmetry molecules, i.e., those that possess fewer than two mutually perpendicular planes of symmetry or rotation axes. In this case, the principal axes of the orientation tensor are not determined by symmetry. With a fixed but otherwise arbitrary molecular axes system x, y, and z, the general orientation factors K_{uv} defined in (21) will now be necessary to describe the uniaxial orientation distribution adequately for measurements of linear dichroism. Only five of them are independent, since the orientation tensor is symmetrical and has a unit trace.

In addition to the five unknown orientation factors, there will be two unknown independent direction cosines for each transition i among the three describing the orientation of the transition moment $\mathbf{M}(i)$ in the molecular framework:

$$\cos M^u(i) = \mathrm{M}_u(i)/|\mathbf{M}(i)|, \qquad u = x, y, z \quad (32)$$

To relate the experimentally determined quantities K_i to our unknowns, we write

$$K_i = \langle \cos^2 M^Z(i) \rangle =$$
$$\langle [\sum_u \cos M^u(i) \cos u^Z][\sum_v \cos M^v(i) \cos v^Z] \rangle \quad (33)$$

and obtain

$$K_i = \sum_{u,v} \cos M^u(i) K_{uv} \cos M^v(i) \quad (34)$$

If the K_i values have been determined for n transitions, there will be n equations of type 34 and $2n + 5$ unknowns. Given the overwhelming number of unknowns, additional information will be needed to solve for any of them. This can have the form of symmetry relations if some symmetry elements are present, in the form of previous knowledge of some transition moment directions, etc. E.g., in the presence of a yz plane of symmetry, $K_{xy} = K_{xz} = 0$, and the three remaining independent unknown K's can be determined from (34) if moment directions are known for three transitions. If one of the principal axes of the orientation tensor is x, the other two can be found by diagonalizing a 2 × 2 matrix with elements K_y, K_{yz} and K_z. Once the principal orientation axes have been found and renamed x, y, and z, with new diagonal orientation factors K_u, (34) simplifies to

$$K_i = \sum_u K_u \cos^2 M^u(\mathrm{i}) \quad (35)$$

With the yz plane of symmetry, the measurement of the K_i value

(18) Matsuoka, Y. *J. Phys. Chem.* **1980**, *84*, 1361.

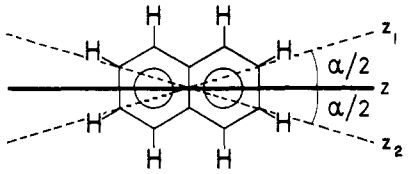

Figure 3. The preferred orientation axes (schematic, dashed lines) and the effective orientation axis (bold line) of naphthalene.

of any additional transition will either show it to be x polarized if $K_i = K_x$ or in-plane polarized if $K_i \geq K_y$. In the latter case, $|M^z(i)|$ can be obtained from

$$\tan^2 M^z(i) = (K_z - K_i)/(K_i - K_y) \qquad (36)$$

Similar simple relations can be derived for other limiting cases. It is now clear that an ability to estimate the orientation factors and the position of the principal orientation axes from molecular shape or other properties for planar aromatic molecules would be highly desirable. It would permit the immediate use of (35) for the determination of polarization directions of π,π^* transitions in low-symmetry aromatics. It is partly with this goal in mind that we have investigated a large group of symmetrical aromatics reported here.

(1.7) The Effective Orientation Axis in a Symmetrical Molecule. For studies of linear dichroism, a uniaxial orientation distribution function of the solute is adequately characterized by the orientation tensor K_{uu}. As seen above, in a suitably chosen system of molecular axes this tensor will be diagonal, and the three diagonal elements, $K_x \leq K_y \leq K_z$, define the average alignment of the x, y, and z axes, respectively, with the Z direction of the sample. The z-axis direction in the molecular framework defined in this fashion has the largest possible value of K; i.e., on the average, it is aligned better with the unique sample axis Z than is any other direction associated with the molecular frame. Similarly, among all directions within the molecule that are perpendicular to z, the one that is aligned the best is y, and finally, the one direction among all possible ones whose average alignment with Z is the worst is x. We refer to the molecular z axis as the effective orientation axis, or orientation axis for short.[8,9]

In symmetrical molecules, the location of the principal orientation axes x, y, and z in the molecular framework is dictated by symmetry except for a possible permutation (if two of them belong to a degenerate representation, a degree of freedom remains; e.g., in benzene any two mutually orthogonal in-plane directions are acceptable for two of the axes). Thus, in the cases considered presently, the only decision that needs to be made is the attribution of the x, y, and z labels to the three molecular axes. As discussed in more detail below, this can be done in virtually all cases by inspection of the molecular shape, using the fact that π,π^* transitions are in-plane polarized.

It is important to note that, in principle, the direction of the effective orientation axis z need not be anywhere near aligned with the unique sample axis Z for any of the solute molecules. We dwell on the concept at some length since considerable confusion on the subject exists in the literature.[4,18] The label "preferred orientation axis" has been proposed[8,9] for those directions in the molecular framework that are nearly aligned with the sample Z axis in a large fraction of the solute molecules. As discussed below, these tend to be the directions of longest molecular dimension or smallest cross section. To take a previously discussed example,[19] naphthalene, the preferred orientation axes may well be the direction connecting carbons 2 and 6 and that connecting carbons 3 and 7, as suggested (Figure 3). We shall refer to them as z_1 and z_2, respectively, and shall label the smaller of the two angles at which they cross as α ($\alpha < \pi/2$). Even in the ideal case in which all naphthalene molecules in an oriented sample are aligned perfectly with their diagonals along the sample Z axis, neither the preferred orientation axis z_1 nor z_2 but rather the symmetry axis z, which bisects α, represents the effective orientation axis. For this hypothetical orientation distribution, we have

$$K_z = \langle \cos^2 z^Z \rangle = \cos^2 (\alpha/2) = (1 + \cos \alpha)/2 \qquad (37)$$

$$K_{z_1} = K_{z_2} = \langle \cos^2 z_1^Z \rangle = (1/2) \cos^2 0 + (1/2) \cos^2 \alpha = (1 + \cos^2 \alpha)/2 \qquad (38)$$

and, since $\cos \alpha > 0$,

$$K_z - K_{z_1} = K_z - K_{z_2} = \cos \alpha \sin^2 (\alpha/2) > 0 \qquad (39)$$

In this calculation it is necessary to recognize that any physical orienting force, however strong, can only orient half of the molecules to line up with their z_1 axis along Z, since molecular symmetry makes z_1 and z_2 physically indistinguishable and the other half of the molecules will therefore be lined up with their z_2 axis along Z. In general, in a symmetrical molecule, the direction of the best average alignment, i.e., the orientation axis, must coincide with or be perpendicular to one of the symmetry axes.

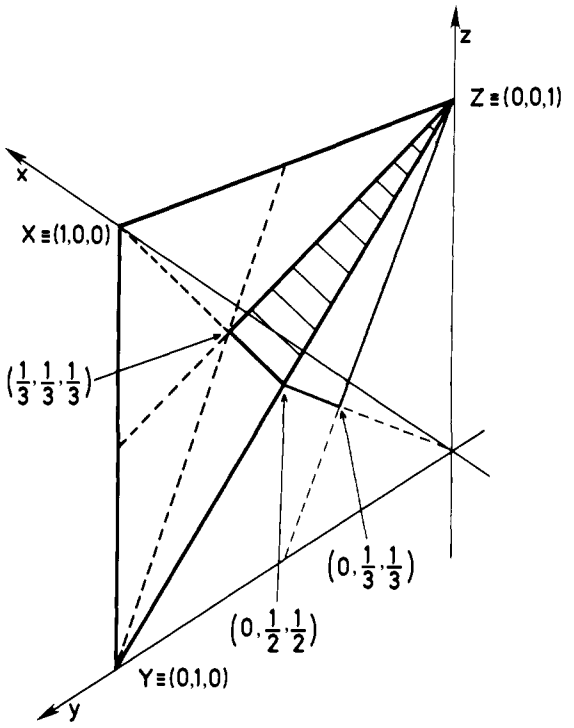

Figure 4. A perspective view of the three-dimensional plot of the allowed combinations of the orientation factors K_x, K_y, and K_z. See text.

2. Description of the Molecular Orientation.

(2.1) The Orientation Triangle. When the orientation factors K_x, K_y, and K_z for a given solute are plotted against each other in a three-dimensional coordinate system, the condition $K_x + K_y + K_z = 1$ restricts the set of points (K_x, K_y, K_z) to a triangular portion of a plane with vertices at points (1, 0, 0) = X, (0, 1, 0) = Y, and (0, 0, 1) = Z, as shown in Figure 4. The vertices correspond to unique orientation distributions: the point U (U = X, Y, or Z) describes a distribution with perfect alignment of the u axis ($u = x$, y, or z, respectively) of all molecules along the unique sample axis (the uniaxial nature of the sample guarantees a random distribution of the other two axes along all directions perpendicular to the sample axis). Every other point in the triangle corresponds to an infinite number of possible orientation distributions that share a particular set of K_z, K_y, and K_x values. It should be noted that points located on the edges of the triangle XYZ in Figure 4 correspond to orientations for which one (or two) K_u's vanish. These orientations are those in which one or two molecular planes such as xy are oriented exactly parallel to the unique axis of the sample for all solute molecules. Such orientation distributions are hardly ever achieved in practice and represent only limiting cases.

(19) Kuball, H.-G.; Altschuh, J.; Schönhofer. A. *Chem. Phys.* **1980**, *49*, 247.

The K_x, K_y, and K_z coordinates of any point in the triangle displayed in Figure 4 can also be visualized in a different way: the distance of the point from that side of the triangle opposite to vertex U is equal to $(3^{1/2}/2)K_u$. Such a mapping of the average squares of the direction cosines inside an equilateral triangle has been used occasionally in the polymer literature.[20]

Once we introduce our axis labeling that leads to $K_z \geq K_y \geq K_x$, points for all possible orientation distributions will lie in a smaller triangle, shaded in Figure 4, whose vertices are (0, 0, 1), ($^1/_3$, $^1/_3$, $^1/_3$), (0, $^1/_2$, $^1/_2$). Since a totally symmetrical treatment of the x, y, and z indices is thus abandoned, one may just as well select only two of the K_u's for the description of the orientation distribution. Since K_y and K_z are the ones directly measured for most aromatic molecules with which we have worked, we arbitrarily select these two and work with a plot of K_z against K_y, i.e., with a projection of the shaded triangle of Figure 4 into the K_yK_z plane. This projected triangle, with vertices (0, 1), ($^1/_3$, $^1/_3$), and ($^1/_2$, $^1/_2$), has been referred to as the orientation triangle in our previous work[3,4,10,16,21] and represents a convenient device for displaying results concerning average molecular orientation. Only one of its vertices, (0, 1), corresponds to a unique orientation distribution. One important distribution among the infinitely many that correspond to the "isotropic" point ($^1/_3$, $^1/_3$) is the totally random distribution; one important distribution among the many that correspond to the vertex ($^1/_2$, $^1/_2$) is characterized by perfect alignment of the yz molecular planes with the unique axis of the sample and by total equivalence of the y and z axes. The line joining the points ($^1/_2$, $^1/_2$) and (0, 1) on the upper side of the small unshaded triangle in Figure 4 corresponds to $K_x = 0$ ($K_z + K_y = 1$) and thus to perfect alignment of the molecular yz plane with the unique sample direction. As a point moves from ($^1/_2$, $^1/_2$) toward (0, 1), the z axis gradually becomes better aligned than the y axis, and in the (0, 1) limit it is aligned perfectly. This line plays an important role in the model of Tanizaki, which assumes that points for all molecules would lie on it when extrapolated to an infinite stretching ratio.[4,22] As mentioned above, points on this line are never observed in real samples of the stretched polymer type. The line from ($^1/_2$, $^1/_2$) to (0, 1) is also assigned special importance in a recent model of Margulies and Yogev.[23] These authors propose that the orientation of aromatic solutes in stretched polyethylene is such that a fraction of the molecules, presumably those contained in the amorphous regions of the polymer, is randomly oriented and the remainder, presumably those contained inside the crystalline regions of the polymer, has a perfectly aligned yz plane. Thus, the first fraction corresponds to the isotropic point ($^1/_3$, $^1/_3$) and the second fraction to a point on the ($^1/_2$, $^1/_2$) to (0, 1) line (the authors actually select one of the infinite number of possible distributions corresponding to the point as being the "true" one). Such a two-fraction distribution function is capable of producing any point in the orientation triangle simply by choosing appropriate weighting factors and is therefore compatible with the experimental results, but so is an infinite number of other orientation functions. The authors point out that their distribution function is also compatible with their measurements of polarized fluorescence. Such compatibility will be shown by an infinite subset of the infinite set of distribution functions that are able to account for the polarized absorption. Clearly, measurements of this type can never prove what the orientation distribution function is; they can only eliminate some of the infinite number of possibilities.[24]

The line joining the points ($^1/_2$, $^1/_2$) and ($^1/_3$, $^1/_3$) on the bottom side of the triangle in Figure 4 corresponds to $K_y = K_z$ and thus to distributions in which the two longer molecular axes, y and z, are equivalent. As a point moves from ($^1/_3$, $^1/_3$) toward ($^1/_2$, $^1/_2$), the yz plane gradually becomes better aligned, and in the ($^1/_2$, $^1/_2$) limit it is aligned perfectly. A position on this line is dictated by symmetry for some molecules. The line joining the points ($^1/_3$, $^1/_3$) and (0, 1) on the right-hand side of the triangle in Figure 4 corresponds to $K_y = K_x$ and thus to distributions in which the two "shorter" axes, x and y, are equivalent. As a point moves from ($^1/_3$, $^1/_3$) toward (0, 1), the z axis gradually aligns better with the unique axis of the sample, and in the (0, 1) limit it is aligned perfectly. Orientations corresponding to a position on the line between ($^1/_3$, $^1/_3$) and (0, 1) are dictated by symmetry in some cases. Points inside the orientation triangle correspond to more general distributions and reflect the continuous nature of a change from one distribution to another.

(2.2) Empirical Relations Between Molecular Shape and Orientation. Figure 5 shows the (K_y, K_z) points for symmetrical aromatic solutes in stretched polyethylene measured at room temperature and referred to the principal axes system; Figure 6 shows similar results for low temperature, in most cases liquid nitrogen temperature. The orientation factors were obtained from linear dichroism in the UV–visible region. Most of the data are new; some have been taken from the literature.[15-17,21,25-27] The accuracy with which the K values can be read from the figures is roughly equal to that of the experimental determinations themselves, and we are therefore not tabulating the numerical values. In most cases, the results for (K_y, K_z) are determined with an error of about ±0.015. In some cases, one of the two K's, frequently K_y, could only be determined with a somewhat higher error limit, and differences in the polyethylene material used in the various experiments have been observed to lead to even higher uncertainties in the relative K values. For instance, in certain polyethylene samples, the point for anthracene (**17**) is located at (K_y, K_z) = (0.20, 0.62), as shown in Figure 2, rather than (0.24, 0.63) as shown in Figure 5 [measurement of IR linear dichroism yields (0.25, 0.64) for the latter sample[28]]. In spite of such uncertainties, the quality of the data is sufficient for a qualitative discussion of possible relations between molecular properties and orientation. Specific comparisons made in the following are always based on comparable measurements. It should be pointed out that higher accuracy can be achieved readily under more strictly controlled conditions, i.e., by using the same batch of polymer for all measurements rather than collecting the data from a series of results obtained over the years. Also, in our experience, measurements of linear dichroism in the IR region yield more accurate results.

The most striking relation that can be observed in Figures 5 and 6 is that between molecular shape and orientation. The molecules used in the study are all planar or nearly so, with the exception of **61**, **85**, and **106**. The largest K_z values are observed for very long and relatively narrow molecules, and the lowest values

(20) Desper. C. R. *J. Appl. Polym. Sci.* **1969**, *13*, 169.
(21) Thulstrup, E. W.; Michl, J. *J. Am. Chem. Soc.* **1976**, *98*, 4533.
(22) Tanizaki, Y.; Kubodera, S.-I. *J. Mol. Spectrosc.* **1967**, *24*, 1. Hiratsuka, H.; Tanizaki, Y.; Hoshi. T. *Spectrochim. Acta, Part A* **1972**, *28*, 2375.
(23) Margulies, L.; Yogev. A. *Chem. Phys.* **1978**, *27*, 89. Aviv, G.; Margulies, L.; Sagiv, J.; Yogev, A.; Mazur. Y. *Spectrosc. Lett.* **1977**, *10*, 423.
(24) The discussion given in ref 23 is somewhat confusing since the sin β factor in the volume element in the Euler angle space $d\Omega = (^1/_8\pi^2) \sin\beta\, d\alpha\, d\beta\, d\gamma$ is considered to be a part of the distribution function. As a result, a constant distribution function does not correspond to a uniform distribution, etc.

(25) Thulstrup, E. W. Thesis, Aarhus University, 1966. Michl, J.; Eggers, J. H. *Tetrahedron* **1974**, *30*, 813. Muller, J. F.; Cagniant, D.; Chalvet, O.; Lavalette, D.; Kolc, J.; Michl, J. *J. Am. Chem. Soc.* **1974**, *96*, 5038. Michl, J.; Thulstrup, E. W.; Eggers, J. H. *Ber. Bunsenges. Phys. Chem.* **1974**, *78*, 575. Nordén, B.; Håkansson, R.; Pedersen, P. B.; Thulstrup, E. W. *Chem. Phys.* **1978**, *33*, 355. Jørgensen, N. H.; Pedersen, P. B.; Thulstrup, E. W.; Michl, J. *Int. J. Quantum Chem, Quantum Chem. Symp.* **1978**, *12*, 419. Plummer, B. F.; Michl, J. *J. Org. Chem.* **1982**, *47*, 1233.
(26) Kolc, J.; Thulstrup, E. W.; Michl, J. *J. Am. Chem. Soc.* **1974**, *96*, 7188. Kolc, J.; Michl, J. *Ibid.* **1976**, *98*, 4540.
(27) Thulstrup, E. W.; Case, P. L.; Michl, J. *Chem. Phys.* **1974**, *6*, 410. Thulstrup, E. W.; Michl, J.; Jutz, C. *J. Chem. Soc., Faraday Trans. 2* **1975**, *71*, 1618. Bischof, P.; Gleiter, R.; Hafner, K.; Kobayashi, M.; Spanget-Larsen, J. *Ber. Bunsenges. Phys. Chem.* **1975**, *79*, 128. Gleiter, R.; Spanget-Larsen, J.; Thulstrup, E. W.; Murata, I.; Nakasuji, K.; Jutz, C. *Helv. Chim. Acta* **1976**, *59*, 1459. Thulstrup, E. W.; Michl, J. *J. Mol. Spectrosc.* **1976**, *61*, 203. Haider, R. Thesis, Technische Hochschule Darmstadt, 1977. Spanget-Larsen, J.; Gleiter, R.; Haider, R.; Thulstrup, E. W. *Mol. Phys.* **1977**, *34*, 1049. Spanget-Larsen, J.; Gleiter, R.; Kobayashi, M.; Engler, E. M.; Shu, P.; Cowan D. O. *J. Am. Chem. Soc.* **1977**, *99*, 2855. Thulstrup, E. W.; Downing, J. W.; Michl, J. *Chem. Phys.* **1977**, *23*, 307. Bartetzko, R.; Gleiter, R. *Angew. Chem.* **1978**, *90*, 481. Dahlgren, T.; Davidsson, Å.; Glaus, J.; Gronowitz, S.; Nordén, B.; Pedersen, P. B.; Thulstrup, E. W. *Chem. Phys.* **1979**, *40*, 397. Spanget-Larsen, J.; Gleiter, R., personal communication.
(28) Radziszewski, J. G.; Michl, J., unpublished results.

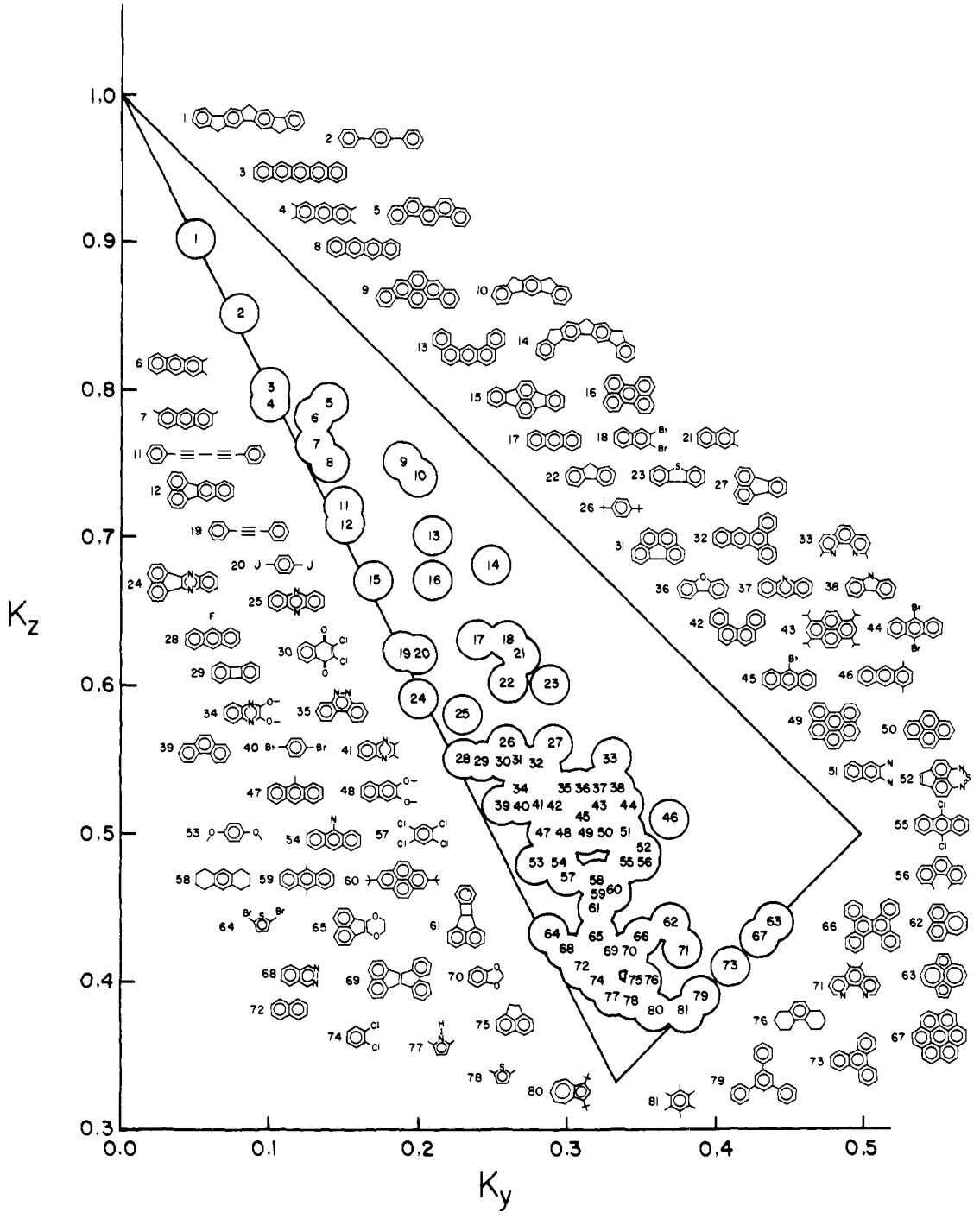

Figure 5. Orientation factors of aromatic molecules in stretched polyethylene at room temperature. The formulas are oriented with their effective orientation axis z horizontal and with the y axis vertical (for **61**, y is the short axis of naphthalene; cf. ref 16). Most of the data are new; some originate in ref 15, 16, 21, 25, and 26.

are found for smaller molecules with their two larger dimensions more or less equal. Molecules that are approximately rod-shaped tend to be close to the left side of the triangle, corresponding to $K_x = K_y$ (in the case of **106** this is demanded by molecular symmetry), disk-shaped molecules are found on the bottom side of the triangle, which corresponds to $K_z = K_y$ (in the case of **81**, **79**, **73**, and **67**, this is dictated by symmetry). Wide planar molecules that have rectangular rather than ellipsoidal shapes such that "their corners are well filled" tend to be relatively close to the upper-right-hand side of the triangle, which corresponds to perfect alignment of the yz molecular plane, $K_z = 1 - K_y$, $K_x = 0$. Qualitatively, these observations may be summarized by stating that for approximately planar molecules, an increase in the molecular dimension along direction u causes an increase in the value of K_u.

Various attempts to establish a quantitative relation between molecular shape and orientation have been made over the years. Popov[29] suggested that the orientation could be directly related to the molecular length divided by the width. Figures 5 and 6 show that this relation is not fulfilled. As pointed out in ref 9, pyrene (**50**) and perylene (**16**) have almost identical lengths and widths, but their orientation in stretched polyethylene at room temperature corresponds to $(K_y, K_z) = (0.32, 0.50)$ and $(0.21, 0.67)$, respectively. A similar comparison can be made for derivatives of naphthalene (**72**), 2,3-dimethylnaphthalene (**21**) (0.27, 0.62), and 2,3-diaminonaphthalene (**51**) (0.34, 0.50) at room temperature and for the **93** (0.20, 0.64) and **88** (0.20, 0.74) pair, both at liquid nitrogen temperature. For the last two compounds,

(29) Popov, K. R. *Opt. Spectrosk.* **1975**, *39*, 285.

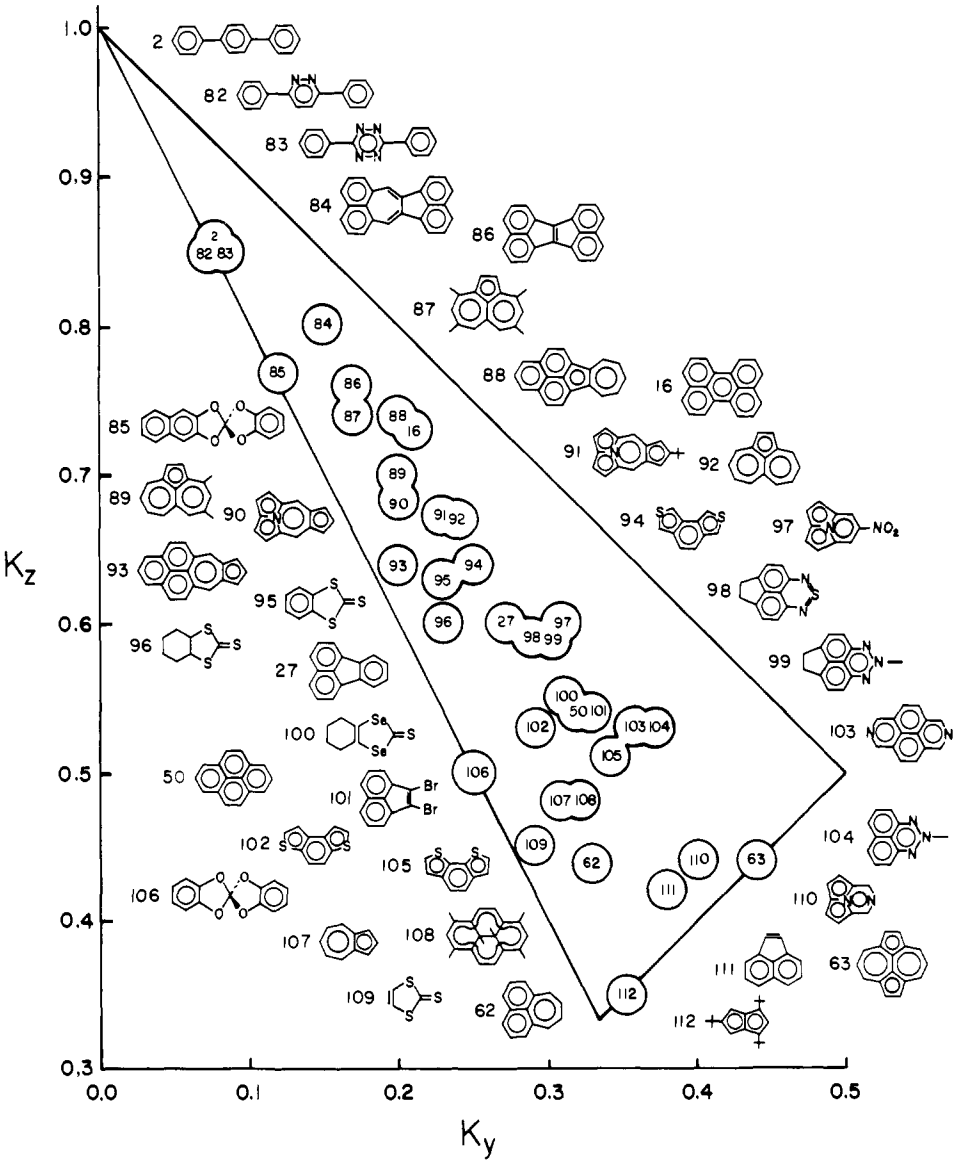

Figure 6. Orientation factors of aromatic molecules in stretched polyethylene at low temperature (see text). The formulas are oriented with their effective orientation axis z horizontal and with the y axis vertical (the x and y axes are equivalent in the nonplanar **85** and **106**). Some of the data are new; most originate in ref 16, 17, 26, and 27.

as well as for pyrene and perylene, the one that "fills its corners" best has the better alignment. Further examples and a discussion of the relation between molecular shape and orientation are given in ref 30.

An attempt to describe the solute orientation as a result of dispersion interaction with the polymer matrix resulted in expressions relating the orientation constants to the anisotropy of the solute polarizability.[31] The agreement between the results of this model and experiment was not quite satisfactory, nor were reliable data on polarizabilities available for a large number of molecules of interest. A later study[32] concluded that the solute orientation cannot be described primarily as a result of attractive forces between solute and solvent, but a new quantitative model based on all three molecular dimensions of the solute molecules did not lead to any significant improvement in the agreement with experiment.[32]

It is interesting to note that the increase in the "out-of-plane" molecular dimension when going from unsaturated to saturated rings leads to the intuitively expected increase in K_x. However, this seems to happen solely at the expense of K_z, while K_y increases or remains constant. Examples from Figure 5 are anthracene (**17**) for which $(K_y, K_z) = (0.24, 0.63)$, compared with (0.32, 0.47) for **58**, and phenanthrene (**39**) for which $(K_y, K_z) = (0.26, 0.52)$, compared with (0.35, 0.40) for **76**.

The changes in orientation caused by heteroatoms in conjugated molecules seem to be somewhat random. In some cases, the replacement of CH by N has little effect on the orientation; in other cases, the effect is very clear (Figure 7). Examples of the first kind are terphenyl (**2**) and some of its aza derivatives (**82**, **83**) that at liquid nitrogen temperature all have orientation distribution functions corresponding to $(K_y, K_z) = (0.08, 0.85)$. It may be noted that this does not necessarily mean that the three orientation distributions are the same, only that their second moments are. Other examples of small orientational effects due to aza replacement in hydrocarbons are found for **39** and **35**, for which (K_y, K_z) are (0.26, 0.52) and (0.30, 0.53), respectively, and for **48** and **34**, $(K_y, K_z) = (0.29, 0.50)$ and (0.27, 0.53), respectively, all at room temperature. These examples lend support to the belief that shape is the only determining factor for the orientation. However, a number of other examples indicate that the situation is not that simple. It has been known for a long time that aza replacement in anthracene (**17**) has a noticeable effect on the orientation.[8] The (K_y, K_z) values for **17**, **37**, and **25** are

(30) Bott, C. C.; Kurucsev, T. *J. Chem. Soc., Faraday Trans. 2* **1975**, *71*, 749.
(31) Lamotte, M. *J. Chim. Phys., Phys.-Chim. Biol.* **1975**, *71*, 803.
(32) Bott, C. C.; Kurucsev, T. *Chem. Phys. Lett.* **1978**, *55*, 585.

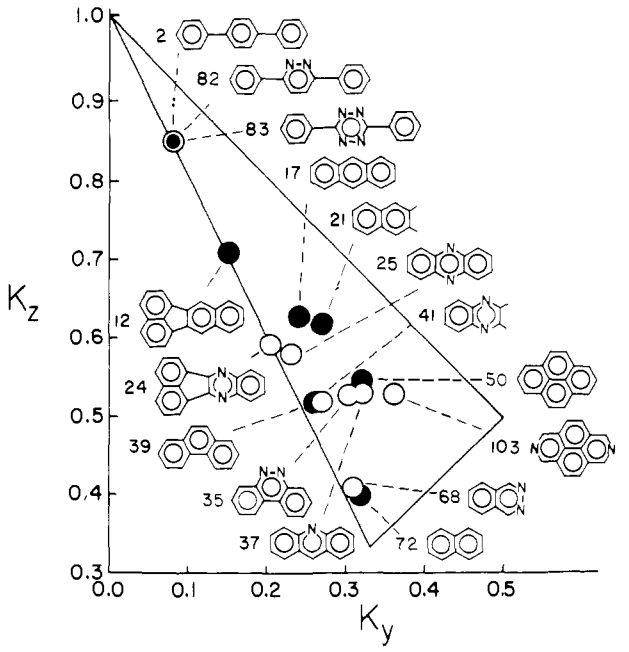

Figure 7. Orientation factors of aromatic hydrocarbons and their aza analogues in stretched polyethylene.

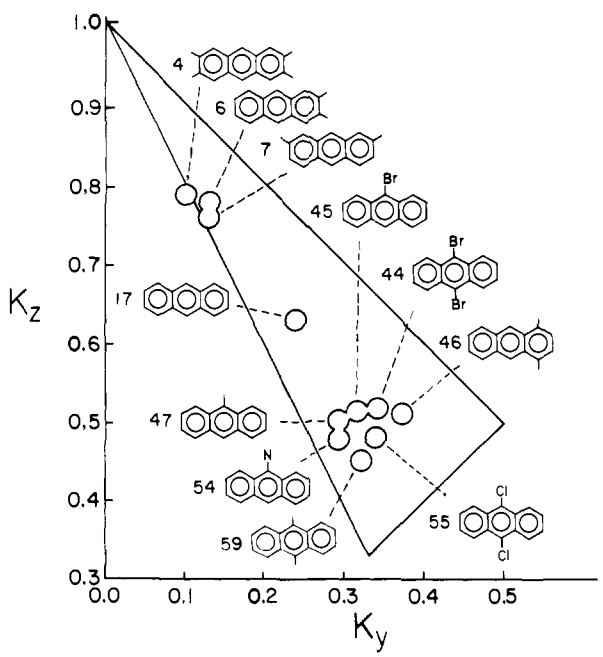

Figure 8. Orientation factors of anthracene derivatives in stretched polyethylene at room temperature (all points were measured by using the same batch of polymer).

(0.24, 0.63), (0.32, 0.53), and (0.23, 0.58), respectively. Other examples of large changes of orientation upon aza replacement are found in **21** and **41** for which (K_y, K_z) are (0.27, 0.62) and (0.27, 0.52), respectively, and **12** and **24**, which have (K_y, K_z) = (0.15, 0.71) and (0.20, 0.59), respectively.

The influence of substituents on the orientation is more clearly related to their effect on the molecular shape. Values of (K_y, K_z) for a number of methyl and halogen substituted anthracenes are shown in Figure 8. They were not all obtained by using the same polyethylene sample but the differences among them are so large that a meaningful discussion is still possible. Among the dimethylanthracenes, 2,3-dimethylanthracene (**6**) obtains the best alignment, (K_y, K_z) = (0.13, 0.78), closely followed by the 2,7-dimethyl derivative (**7**) with the values (0.13, 0.76). Both these compounds are far better aligned than anthracene (**17**) itself, with (K_y, K_z) = (0.24, 0.63), but not as well as 2,3,6,7-tetramethylanthracene (**4**), with (K_y, K_z) = (0.10, 0.79). On the other hand, the 1,4-dimethyl derivative (**46**), with (K_y, K_z) = (0.37, 0.51), is aligned considerably worse than anthracene itself, but still better than the 9,10-dimethyl derivative (**59**), which has (K_y, K_z) = (0.32, 0.46). This molecule clearly does not fill its corners well.

Other substituents have effects similar to those of methyl. Thus, 9,10-dibromoanthracene (**44**) also aligns worse than anthracene itself, (K_y, K_z) = (0.34, 0.52). This alignment is better than that of **59**, mentioned above, and similar to that of 9,10-dichloroanthracene (**55**), (K_y, K_z) = (0.34, 0.48), but the reasons for this do not seem to be directly related to molecular shape. A comparison of 9,10-disubstituted and 9-monosubstituted anthracenes is also given in Figure 8. For the bromo and methyl monosubstituted compounds, **45** and **47**, respectively, the alignment is similar as in the case of the disubstituted compounds mentioned above: (K_y, K_z) = (0.31, 0.51) for Br and (0.29, 0.50) for CH_3.

In all molecules studied so far for which absolute polarization directions have been determined from single-crystal or other absolute measurements, the molecular long axis has been the z axis, that is, has had the largest value of K. For instance, acenaphthylene (**111**), which has an alignment at low temperature corresponding to (K_y, K_z) = (0.38, 0.42), has the z axis along the longer dimension, perpendicular to the symmetry axis of the molecule. However, in 1,2-dibromoacenaphthylene (**101**), the symmetry axis corresponds to the longer dimension, and the experimental results[21] show that the z axis now lies along this direction, perpendicular to its direction in the parent hydrocarbon. The K values obtained are (K_y, K_z) = (0.33, 0.54). For the planar molecules compared so far, the lowest K value has always been obtained for the direction perpendicular to the molecular plane, usually by using $K_x = 1 - K_y - K_z$.

The fact that the alignments in stretched polyethylene have been such that the z axes coincide with the long axis of the molecule in all cases in which absolute data are available makes it tempting to use the stretched-sheet method itself as an absolute method for planar or nearly planar molecules. This seems clearly justified in those cases in which the molecular dimensions are not very close to each other. However, this result should not be blindly extrapolated to other polymers in which different kinds of solvent–solute interactions may dominate.

The situation is undoubtedly more complex for highly nonplanar molecules such as **61**. In **61**, the orientation axis z lies along an axis that is perpendicular to the longest dimension of the molecule.[16] In molecules of this type, the direction of the longest dimension need not coincide with the direction along which the molecule has the smallest cross section, and it is quite likely that the latter criterion[8] should be used in defining the "long axis" of the molecule.

(2.3) Temperature Effects. A number of molecules have been studied both at room and low temperature, as shown in Figures 5 and 6. Here, low temperatures mean either those obtained by immersing the polymer sheet into liquid nitrogen, placing it in a Dewar vessel just above a liquid nitrogen surface, or the even lower ones, which have been obtained in a closed-cycle helium cryostat. A comparison of results for K values obtained at room and low temperatures shows that the alignment in almost all cases is improved (K_x decreases) when the temperature is reduced. In some cases, the z axis becomes better aligned (K_z increases), in other cases, the increase is observed for K_y or for both K_y and K_z. Figure 9 shows a comparison for a number of molecules of the results obtained at different temperatures.

Conclusions

Figures 5 and 6 leave no doubt that the orientation factors of planar or nearly planar solutes in stretched polyethylene are governed primarily (but not solely) by the solute shape. This makes the stretched-sheet method of determination of transition-moment directions absolute for this important class of molecules. The ability to roughly estimate the orientation factors K from molecular shape opens a way to reliable—even if not highly accurate—determinations of polarization directions in aromatic molecules of lower symmetry and of reduced spectra for symmetrical molecules for which the determination of two K values

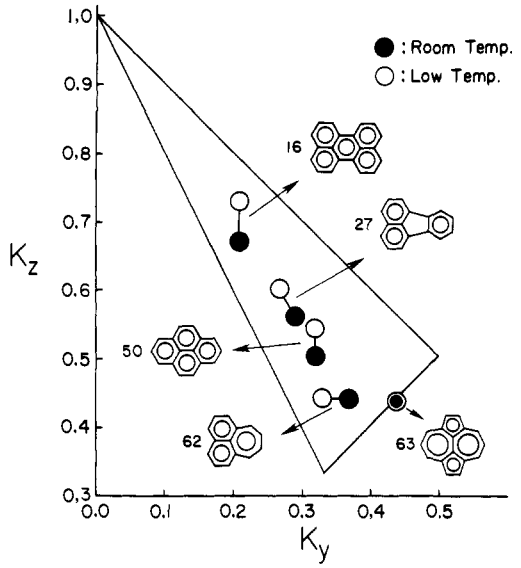

Figure 9. Orientation factors of selected hydrocarbons at room and at low temperatures (see text).

has not been possible from the observed spectra.

The main advantage of the method is its extreme simplicity, which now makes the determination of absolute polarization directions of electronic and vibrational transitions in most aromatic molecules a trivial task. The main shortcoming of the method is its purely empirical nature. The detailed mechanism of the orientation effect of stretched polyethylene can only be established through additional work, but the data base presented here can serve as a useful set of test cases against which more detailed models of orientation can be evaluated.

Acknowledgment. This work was supported by the U.S. Public Health Service (GM-19450), the U.S. Army Research Office (DAAG29-82-K-0024), and the Danish Natural Science Research Council. Technical assistance of Ludmila Jonas is gratefully acknowledged.

Registry No. 1, 28820-47-5; **2**, 92-94-4; **3**, 135-48-8; **4**, 15254-25-8; **5**, 213-46-7; **6**, 613-06-9; **7**, 782-23-0; **8**, 92-24-0; **9**, 189-55-9; **10**, 525-18-8; **11**, 886-66-8; **12**, 207-08-9; **13**, 224-41-9; **14**, 23913-06-6; **15**, 193-43-1; **16**, 198-55-0; **17**, 120-12-7; **18**, 13214-70-5; **19**, 501-65-5; **20**, 624-38-4; **21**, 581-40-8; **22**, 86-73-7; **23**, 132-65-0; **24**, 207-11-4; **25**, 92-82-0; **26**, 1012-72-2; **27**, 206-44-0; **28**, 529-85-1; **29**, 259-79-0; **30**, 117-80-6; **31**, 203-12-3; **32**, 215-58-7; **33**, 484-11-7; **34**, 6333-43-3; **35**, 230-17-1; **36**, 132-64-9; **37**, 260-94-6; **38**, 86-74-8; **39**, 85-01-8; **40**, 106-37-6; **41**, 2379-55-7; **42**, 195-19-7; **43**, 24300-95-6; **44**, 523-27-3; **45**, 1564-64-3; **46**, 781-92-0; **47**, 779-02-2; **48**, 10103-06-7; **49**, 191-24-2; **50**, 129-00-0; **51**, 771-97-1; **52**, 4145-24-8; **53**, 150-78-7; **54**, 779-03-3; **55**, 605-48-1; **56**, 3674-69-9; **57**, 95-94-3; **58**, 1079-71-6; **59**, 781-43-1; **60**, 24300-91-2; **61**, 28172-99-8; **62**, 208-20-8; **63**, 193-85-1; **64**, 3141-27-3; **65**, 81626-25-7; **66**, 191-68-4; **67**, 191-07-1; **68**, 253-52-1; **69**, 13638-84-1; **70**, 274-09-9; **71**, 3002-81-1; **72**, 91-20-3; **73**, 217-59-4; **74**, 95-50-1; **75**, 83-32-9; **76**, 5325-97-3; **77**, 625-84-3; **78**, 638-02-8; **79**, 612-71-5; **80**, 16458-17-6; **81**, 87-85-4; **82**, 891-22-5; **83**, 6830-78-0; **84**, 20343-16-2; **85**, 82823-46-9; **86**, 340-99-8; **87**, 17597-70-5; **88**, 54100-60-6; **89**, 20672-23-5; **90**, 27884-38-4; **91**, 82823-47-0; **92**, 209-42-7; **93**, 6580-41-2; **94**, 23062-31-9; **95**, 934-36-1; **96**, 2164-87-6; **97**, 27884-37-3; **98**, 4039-37-6; **99**, 15881-33-1; **100**, 82823-48-1; **101**, 13019-33-5; **102**, 210-80-0; **103**, 194-00-3; **104**, 40237-01-2; **105**, 211-53-0; **106**, 181-82-8; **107**, 275-51-4; **108**, 32495-80-0; **109**, 930-35-8; **110**, 27884-36-2; **111**, 208-96-8; **112**, 50356-52-0; polyethylene, 9002-88-4.

Temperature Dependence of Excimer Formation between Pyrenes at the Ends of a Polymer in a Good Solvent. Cyclization Dynamics of Polymers. 8†

A. E. C. Redpath and M. A. Winnik*

Contribution from the Lash Miller Laboratories, Department of Chemistry, and Erindale College, University of Toronto, Toronto, Ontario, Canada M5S 1A1. *Received February 4, 1982*

Abstract: The kinetics of intramolecular pyrene excimer formation have been studied in dilute toluene solution as a function of temperature for polystyrene molecules capped on both ends with pyrene groups. Three samples, of $\bar{M}_n$ 3900, 6600, and 9200, were examined. The cyclization rate constant $\langle k_1 \rangle$ was sensitive to chain length and had an E_a of 3.4 kcal/mol. Excimer dissociation back to locally excited pyrene (k_{-1}) was *insensitive* to chain length and had an E_a = 10.4 kcal/mol. Hence for these polymers, the $\Delta H°$ for pyrene excimer formation is 7 kcal/mol, very similar to that of pyrene itself.

Since the initial report in 1965 by Hirayama,[1] numerous reports have appeared describing intramolecular excimer formation in bichromophoric molecules and intramolecular exciplex formation between different groups at the ends of short-chain molecules.[2] These phenomena are of interest for a variety of reasons. With these molecules one can explore how the stereochemical constraints of the chain affect excimer and exciplex spectroscopy. In other instances, these kinds of molecules permit one to study interactions between pairs of chromophores at high dilution. Our interest is in the shape and motion of polymer chains. When one studies intramolecular cyclization between groups at the ends of long polymer chains, one can in principle obtain information about chain conformation and chain dynamics. These inferences depend

Scheme I

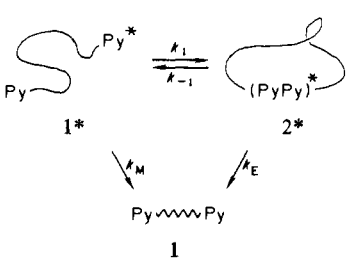

† This paper is dedicated to Mr. Schuster of the Centre de Recherches sur les Macromolécules in Strasbourg, France, on the occasion of his retirement.

0002-7863/82/1504-5604$01.25/0